








RESEARCH ARTICLE | JANUARY 09 2023

Sign reversal of planar Hall effect with temperature in La-doped Sr₂IrO₄ films

Special Collection: [Metal Oxide Thin-Film Electronics](#)

Mingrui Liu ; Jianing Yue ; Jianchao Meng; Tingna Shao; Chunli Yao; Xiaojuan Sun ; Jiakai Nie  ; Dabing Li  

 Check for updates

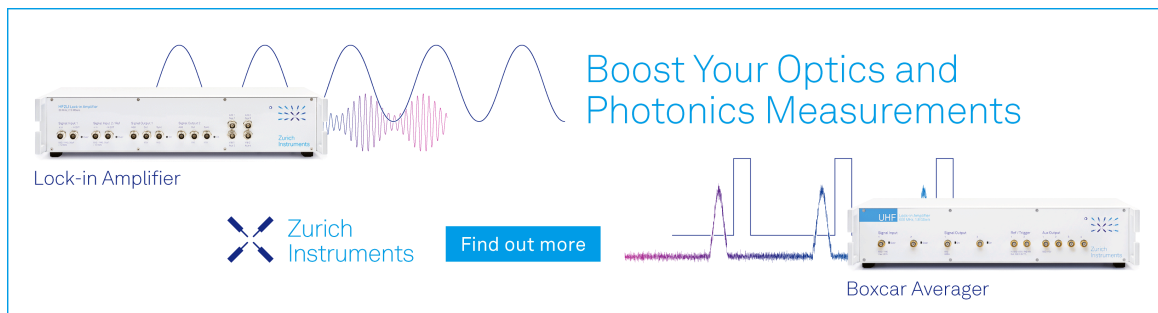
Appl. Phys. Lett. 122, 022402 (2023)

<https://doi.org/10.1063/5.0134002>




CrossMark

Boost Your Optics and Photonics Measurements



Lock-in Amplifier

 Zurich Instruments

[Find out more](#)

Boxcar Averager

Sign reversal of planar Hall effect with temperature in La-doped Sr_2IrO_4 films

Cite as: Appl. Phys. Lett. **122**, 022402 (2023); doi: [10.1063/5.0134002](https://doi.org/10.1063/5.0134002)

Submitted: 7 November 2022 · Accepted: 29 December 2022 ·

Published Online: 9 January 2023



View Online



Export Citation



CrossMark

Mingrui Liu,¹ Jianing Yue,² Jianchao Meng,³ Tingna Shao,² Chunli Yao,² Xiaojuan Sun,¹ Jiakai Nie,^{2,a)} and Dabing Li^{a)}

AFFILIATIONS

¹State Key Laboratory of Luminescence and Applications, Changchun Institute of Optics, Fine Mechanics and Physics, Chinese Academy of Sciences, Changchun 130033, China

²Department of Physics, Beijing Normal University, Beijing 100875, People's Republic of China

³College of Science, Inner Mongolia University of Technology, Hohhot 010051, People's Republic of China

Note: This paper is part of the APL Special Collection on Metal Oxide Thin-Film Electronics.

^{a)}Authors to whom correspondence should be addressed: jcnie@bnu.edu.cn and lidb@ciomp.ac.cn

ABSTRACT

Electron-doped Sr_2IrO_4 is the best candidate for unconventional superconductivity, but direct evidence of superconductivity has not been experimentally confirmed. Therefore, it is urgent to explore the complex and rich physical properties caused by doping. The planar Hall effect (PHE) is a sensitive technique for the characterization of intrinsic magnetic properties in magnetic thin films and is applied widely in spintronic devices. In this work, the PHE for La-doped Sr_2IrO_4 films as a function of the magnetic field direction and temperature exhibited unique properties caused by electron doping. The amplitude of PHE is proportional to the strength of the applied magnetic field. Remarkably, as the temperature increased, a sign reversal of angle-dependent PHE occurred at 90 K, which indicated the change of magnetic anisotropy. Subsequent variable-temperature traditional Hall measurements and time-resolved optical studies eliminated different types of carrier interactions. The anisotropic magnetoresistance measurements indicated that the sign reversal can be attributed to the changes of a spin structure after electron doping, and the reversal temperature is related to the strength of ferromagnetism. These results provide a platform to study the magnetic interactions and suggest the possibility of realizing thermal controllable magnetic sensor devices in electron-doped Sr_2IrO_4 films.

Published under an exclusive license by AIP Publishing. <https://doi.org/10.1063/5.0134002>

Due to the fact that magnitude of spin-orbit coupling (SOC) is proportional to the fourth power of the atomic number,¹ 5d transition metal oxides (TMOs) have strong SOC interactions, which excite more abundant quantum states such as topological insulators,² Weyl semimetals,³ and quantum spin liquids,⁴ providing a broad platform for the development and application of new materials. Among these 5d TMOs, layered perovskite Sr_2IrO_4 is of particular significance. The similarity with cuprates in terms of electronic and lattice structures make Sr_2IrO_4 a good candidate for exploring unconventional high-temperature superconductors by electron doping.^{5,6} However, there has been no direct confirmation of superconductivity yet despite intensive experimental efforts, such as La substitution,^{7–12} oxygen deficiency,¹³ and surface K dosing,¹⁴ which has led to various unresolved issues related to this material. It is generally hypothesized that magnetic fluctuation is the primary pairing glue in cuprate superconductors.¹⁵ Hence, studying the magnetic

properties of electron-doped Sr_2IrO_4 may provide a prospective platform to better understand this system.

In Sr_2IrO_4 , the spin of Ir^{4+} is in an antiferromagnetic arrangement, but because of the rotation of the IrO_6 octahedron, a net magnetic moment exists in each IrO_2 layer,^{16,17} and the spin-flip transition can be triggered by applying a small magnetic field in the ab plane, resulting in a weak ferromagnetic phase¹⁸ (see Figs. S1(a) and S1(b) in the [supplementary material](#)). Doping of La will reduce the rotation angle of the IrO_6 octahedra (δ)⁸ and transform magnetic Ir^{4+} ions into nonmagnetic Ir^{3+} ions due to the introduction of electrons,⁹ which lead to the reduction of ferromagnetism. DC-MT measurements in the [supplementary material](#) [Fig. S1(c)] show that both the magnetization and T_N decrease after La doping. However, the ferromagnetism of La-doped Sr_2IrO_4 films with a nanoscale is further weakened; therefore, it is difficult to subtract the magnetic contribution of the substrate by traditional magnetometry techniques, such as

vibrating sample magnetometry (VSM), which hinders the study of the magnetic properties for La-doped Sr_2IrO_4 films [Fig. S1(d) in the [supplementary material](#)].

Recently, magneto-transport measurements, such as the anisotropic magnetoresistance (AMR), have emerged as a popular tool for studying magnetic interactions in Sr_2IrO_4 films.^{19–21} In addition, as a twin effect of AMR, the planar Hall effect (PHE) is a more sensitive technique to characterize the intrinsic magnetic properties and has remarkable advantages for applications to spintronic devices because of lower thermal drift,²² higher signal-to-noise ratio,²³ and sensitivity to the direction of magnetization.²⁴ In the PHE, the directions of the magnetic field and current are applied in the same plane, a transverse voltage can be detected due to the interaction between the magnetization and current in the plane of the film, and the transverse resistance R_{xy} can be expressed as follows:

$$R_{xy} = \frac{1}{2}(\Delta R) \sin 2\psi, \quad \Delta R = R_{//} - R_{\perp}, \quad (1)$$

where $R_{//}$ and R_{\perp} are the resistances when the current is, respectively, parallel and perpendicular to the magnetization and ψ is the angle between the directions of magnetization and current.²⁵ ΔR could be either positive or negative depending on the magnetic anisotropy related to s - d scattering and SOC,^{26–28} which plays an important role in studying the detailed scattering process and the change of spin structure.^{29,30} The previous work has reported the magnetic field controllable PHE in undoped Sr_2IrO_4 films,³¹ but the PHE in electron-doped Sr_2IrO_4 films has not been systematically studied. Therefore, studying the PHE of electron-doped Sr_2IrO_4 films may provide a prospective platform to better understand this system and promote its application in spintronic devices.

In this paper, a “sinusoidal-shaped” PHE was observed in La-doped Sr_2IrO_4 films at various temperatures and magnetic fields. The amplitude of R_{PHE} is proportional to the strength of magnetic fields at a fixed temperature. Furthermore, with increasing temperature, a sign reversal of PHE occurred at 90 K. Since the sign of PHE is related to $R_{//}$ and R_{\perp} , the sign reversal indicates that the magnetic anisotropy of the La-doped Sr_2IrO_4 film changes at 90 K. Traditional hall measurements and time-resolved optical studies for variable temperatures indicate that there is no change in the type of carriers around 90 K, excluding contributions of different types of carrier interactions. Combining in-plane AMR measurements, we propose that the sign reversal of PHE is probably due to changes in the spin structure, and the reversal temperature is related to the strength of ferromagnetism. This work provides a perspective to study the magnetic properties in electron-doped Sr_2IrO_4 films. The response of PHE to the temperature indicates that electron-doped Sr_2IrO_4 may have potential applications in spintronic and thermal switch magnetic sensor devices.

A stoichiometric $\text{La}_{0.05}\text{Sr}_{1.95}\text{IrO}_4$ polycrystalline pellet was used as the target of pulsed laser deposition (PLD). Its ferromagnetism was characterized by DC-MT measurements using VSM [Fig. S1(c) in the [supplementary material](#)]. For PLD deposition, atomically flat TiO_2 -terminated (001) SrTiO_3 (STO) was used as the substrate. A KrF excimer laser ($\lambda = 248$ nm) with a pulse energy density of 0.6 J/cm² at a repetition rate of 1 Hz was used. The substrate temperature was kept at 700 °C, and the oxygen pressure was at 1×10^{-2} mbar. The actual composition of La in the film is 0.07 (S2 in the [supplementary material](#)) owing to the off-stoichiometry issue during PLD growth.

We used an x-ray diffractometer with Cu K- α 1 radiation of wavelength $\lambda = 0.15406$ nm and an atomic force microscope (AFM) to characterize the structure and surface of the film. Furthermore, the La-doped Sr_2IrO_4 film was converted into patterned Hall bar structures by using optical lithography and argon ion etching. The transverse resistances R_{xy} and longitudinal resistances R_{xx} were all measured in the physical properties measurement system (Quantum Design). The magnetic structure of the La-doped Sr_2IrO_4 film was determined by out-of-plane and in-plane AMR before the PHE measurements. As shown in the [supplementary material](#) (Fig. S3), the net moment (easy axis) is along the [110] direction in the plane.

In addition, time-resolved optical studies that are sensitive to the dynamical process of carriers³² were performed at various temperatures. We used a Yb:KGW femtosecond laser source (Light Conversion, Lithuania) to generate laser pulses with a center wavelength of 1030 nm, a repetition rate of 200 kHz, and near 290 fs duration; 80% of the energy was used to pump the collinear optical parametric amplifier (Light Conversion, Lithuania), which generated a pulse of 800 nm as the pump light; 12% of the energy passed through BaB_2O_4 (BBO) to generate a second harmonic pulse as probe light. After passing through the variable delay line, the 2.5 nJ probe light was combined with the 25 nJ pump light and focused on the sample, which was placed in a variable temperature controller. The light reflected by the sample was passed through a low-pass filter to filter out the pump light, the remaining probe light was incident on the avalanche photo-diode (APD, Hamamatsu Photonics), and the transient signal was extracted by the lock-in amplifier (Stanford Research Systems).

Figure 1 shows θ - 2θ x-ray diffraction scans of the sample discussed here. We can identify (00 l) strong peaks of the La-doped Sr_2IrO_4 on STO (001) substrates. The left inset of Fig. 1 shows the significant Laue fringe peaks around the (0012) peak, indicating good epitaxial characteristics. The film thickness determined from the adjacent reflectivity peaks was 28 nm. The right inset of Fig. 1 shows the surface morphological images with roughness within 1 nm.

We initially studied PHE for various magnetic fields at 20 K. The schematic arrangement of the PHE measurement is shown in Fig. 2(a),

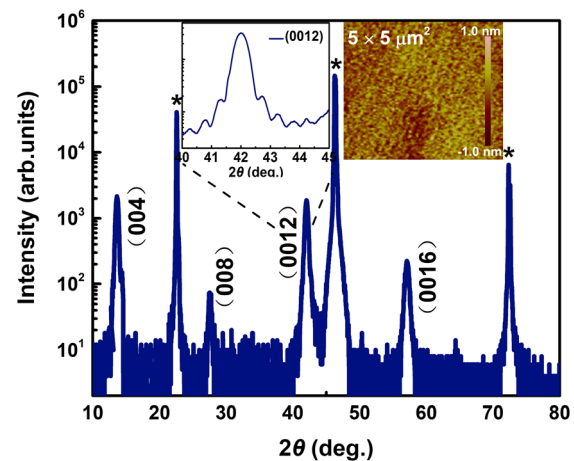


FIG. 1. θ - 2θ x-ray diffraction scans of the La-doped Sr_2IrO_4 film; the diffraction peaks of the STO substrate are represented by asterisks; inset: Laue oscillations around (0012) and surface morphological image.

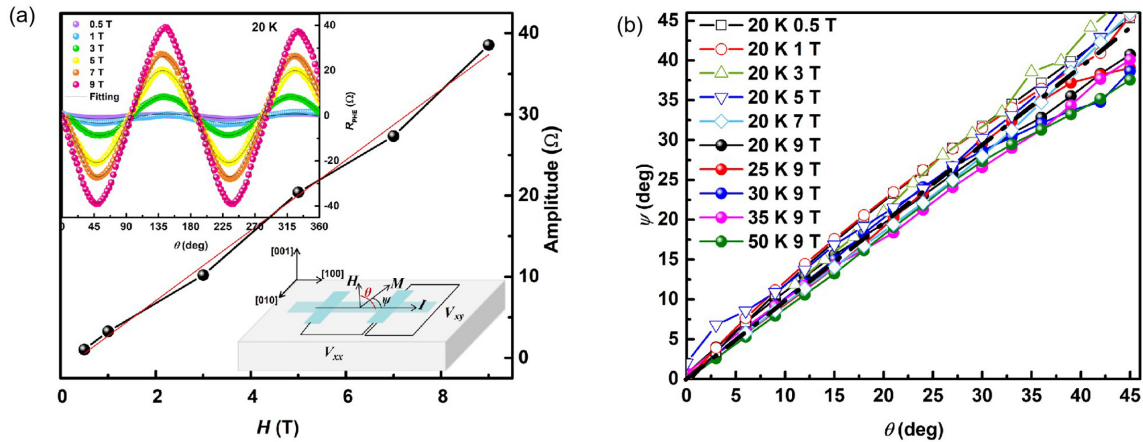


FIG. 2. (a) Amplitude of R_{PHE} as a function of H for La-doped Sr_2IrO_4 films at 20 K and the schematic of R_{PHE} measurements. Inset: Angular dependence of the R_{PHE} in an applied H of 0.5, 1, 3, 5, 7, and 9 T at 20 K. (b) Extracted ψ vs θ for various temperatures and magnetic fields. The black dashed line is a guide for the eyes when $\psi \approx \theta$.

where the dc current I is injected along the $[100]$ direction, the magnetic field H is applied in the plane, θ is the angle between H and I , and ψ is the angle between magnetic moments M and current. We normalized all the R_{xy} measurements in this paper as $R_{xy} = R_{xy}^{raw} - R_{xx} \cdot [R_{xy}^{raw}(0) / R_{xx}(0)]$ ³³ to exclude the contribution of the R_{xx} owing to a slight misalignment of the electrodes, $R(0)$ denotes R_{xy} or R_{xx} at 0 T. The inset of Fig. 2(a) is the angular dependence of R_{PHE} with different magnetic fields, where $R_{PHE} = R_{xy}(\theta) - R_{xy}(0^\circ)$. Compared with the fourfold-symmetric PHE (caused by intrinsic magnetocrystalline anisotropy) in undoped Sr_2IrO_4 films under a low magnetic field,³¹ a sinusoidal-shaped twofold symmetry can be observed from 0.5 to 9 T; it could be well fitted in Eq. (1), which indicates the directions of the applied magnetic field and magnetization approximately coincide. When H is rotated in the plane, the direction of M can be determined based on the Zeeman energy and the magnetic-anisotropy energy.³⁴ The former is proportional to the magnetic field,³⁴ and the latter is dominated by the magnetocrystalline-anisotropy energy, which preferred to align magnetization with the easy axis. We extracted the angle ψ between magnetic moments and current from R_{PHE} as $\psi = 1/2 \sin^{-1}(R_{PHE}/R_{PHE,max})$.³⁴ Figure 2(b) shows the $\psi(\theta)$ extracted within the quadrant $\theta = [0^\circ, 45^\circ]$. $\psi(\theta)$ shows an almost linear relation at various magnetic fields, which further validates that the Zeeman energy dominates the magnetic-anisotropy energy in the La-doped Sr_2IrO_4 film. The difference between the above-mentioned PHEs of undoped Sr_2IrO_4 films and electron-doped Sr_2IrO_4 films at low temperatures and small magnetic fields is attributed to the fact that La doping weakens the ferromagnetism of Sr_2IrO_4 films^{2,30} and further affects its magnetocrystalline anisotropy.

In addition, Fig. 2(a) shows that the amplitude of PHE increases approximately linearly with increasing H , which is attributed to the coupling of the weak ferromagnetic moment and the external field. Due to the strong SOC interaction in $5d$ iridates, the amplitude of PHE for La-doped Sr_2IrO_4 film approaches 40Ω at 9 T, which is comparable with the giant PHE in ferromagnetic semiconductors.^{35,36} [A detailed magnitude comparison with other previously reported materials at 4 T can be seen in the [supplementary material](#) (Fig. S4).]

To gain further insight into PHE, angular-dependent PHE for different temperatures was investigated at 9 T. The obtained PHE

amplitude exhibits a very strong temperature dependence. As presented in Figs. 3(a) and 3(b), PHE shows a weakening trend with increasing temperature. The $\psi(\theta)$ from 20 to 50 K at 9 T is shown in Fig. 2(b). Interestingly, the amplitude of PHE changes its sign at approximately 90 K. According to Eq. (1), the amplitude of PHE is determined by the relative magnitude of $R_{||}$ and R_{\perp} . To quantitatively analyze this sign reversal, we plot the PHE amplitude at $\theta = 45^\circ$ as a function of temperature in Fig. 3(c). This figure shows that the amplitude is negative with $R_{||} < R_{\perp}$ from 20 to 80 K but becomes positive with $R_{||} > R_{\perp}$ above 80 K. It is easy to understand that the magnetic anisotropy decreases with increasing temperature owing to the thermal disturbance. However, the amplitude increases abnormally from 80 to 100 K [the shaded area in Fig. 3(c)]; the sign reversal of PHE also occurs in this temperature zone.

To validate the relative magnitude of $R_{||}$ and R_{\perp} , we fixed the magnetic field at 45° and measured the temperature dependence of the R_{xx} parallel and perpendicular to the magnetic field. The measurement setup is schematically presented in Fig. 3(d); we normalize $R_{xx(\parallel,\tau)}$ as $MR_{(\parallel,\tau)} = [R_{(\parallel,\tau)}(H) - R_{(\parallel,\tau)}(0)] / R_{(\parallel,\tau)}(0) \times 100\%$ to exclude the contribution of the R_{xx} at 0 T. As shown in Fig. 3(d), $MR_{||}$ is significantly smaller than MR_{\perp} at 20 K but exceeds MR_{\perp} above 80 K, which is consistent with the sign reversal in PHE. As the temperature increases further, the magnetic anisotropy between $MR_{||}$ and MR_{\perp} decreases.

Akouala *et al.* have found the PHE with opposite sign in n-type ZnO and p-type CuO, which they attributed to the way in which electrons and holes contribute differently to spin-orbit coupling.²⁶ In this work, doping of La will introduce electrons into p-type Sr_2IrO_4 ,^{19,37} which reveals an interaction between electrons and holes in the La-doped Sr_2IrO_4 film. To investigate whether the change in the dominant carrier type with temperature causes the sign reversal of PHE in the La-doped Sr_2IrO_4 film, we performed traditional Hall measurements for various temperatures. As shown in Fig. 4(a), the orientation of the magnetic field is out of plane and perpendicular to the current. In a magnetic system, the Hall resistivity ρ_{xy} on the applied perpendicular field H can be expressed as $\rho_{xy} = R_0 H + R_s M$.³⁸ The second term represents the anomalous Hall effect contribution due to the spontaneous magnetization. However, there are few reports on the anomalous

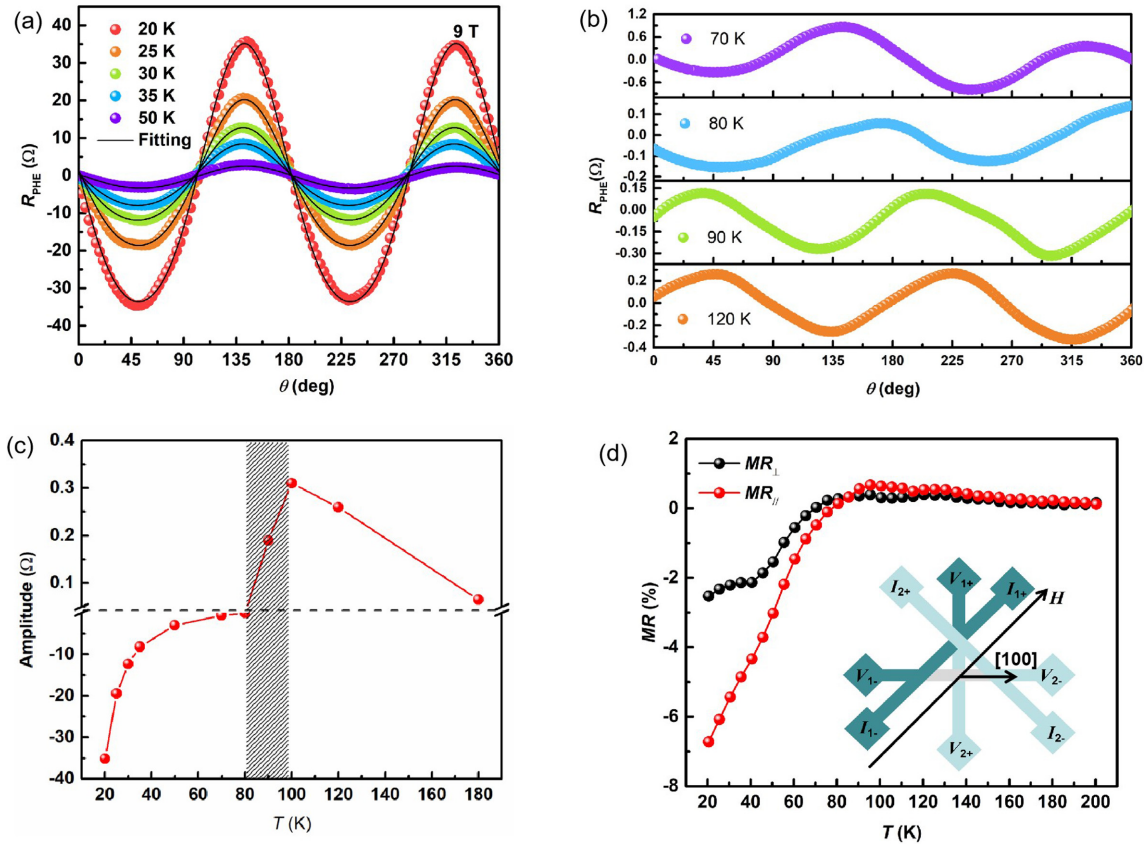


FIG. 3. Measurements of R_{PHE} vs θ at 9 T for various temperatures (a) 20–50 K and (b) 70–120 K. (c) Amplitude of R_{PHE} as a function of temperature for La-doped Sr_2IrO_4 films at 9 T. The shaded area denotes the temperature zone, where PHE shows an abnormal behavior. (d) Temperature-dependent MR at 9 T, the magnetic field is at 45° to the [100] direction, $MR_{(\parallel, \perp)}$ is the normalized $R_{xx(\parallel, \perp)}$ when the current is parallel (I_{1+} , I_{1-}) and perpendicular (I_{2+} , I_{2-}) to the magnetic field.

Hall effect of La-doped Sr_2IrO_4 films due to the fact that canted ferromagnetism is weak. We did not observe the hysteresis of the Hall curve around 0 T when scanning the magnetic field in reverse (not shown), suggesting a weak contribution from the anomalous Hall effect. The nonlinearity of the Hall curve in Fig. 4(a) is due to the fact that poor conductivity causes fluctuations in data points during testing especially at low temperatures. As shown in the inset of Fig. 4(a), the sample exhibits semiconducting temperature dependence below 300 K. The resistivity increases with decreasing temperature and is out of range below 15 K. Furthermore, the resistivity can be well fitted using a 3D Mott-variable range hopping mechanism $\rho = \rho_0 \exp(\frac{T_M}{T})^{\frac{1}{4}}$,³⁹ which indicates there is no transition of a conduction mechanism from 15 to 300 K. Here, ρ_0 is the resistivity coefficient, and T_M is the characteristic temperature. Considering the negative slope of traditional Hall resistance R_{xy} vs the magnetic field, electrons are the dominant carrier from 35 to 300 K, and there is no change in the dominant carrier type around 90 K. [The sheet carrier density n_s and carrier mobility μ are calculated and plotted as a function of temperature in the supplementary material (Fig. S5).].

Furthermore, we performed time-resolved optical studies to better understand the effect of temperature on carrier dynamics. As shown in Fig. 4(b), the excited state dynamics at different temperatures

all show a slow rise and no obvious change around 90 K, indicating that the dominant carrier type does not change with temperature, which corroborate the observations from the traditional Hall measurements. Therefore, we assert that the sign reversal of PHE in the La-doped Sr_2IrO_4 film is independent of the carrier type.

Because PHE is sensitive to the intrinsic magnetism, previous studies found that the change in the spin structure can also lead to the sign reversal of PHE.^{28,29,40} In our previous work about undoped Sr_2IrO_4 films, the PHE amplitude is negative when the angle θ between the magnetic field H and current I is 45° , and there is no sign reversal of PHE for various temperatures at 9 T.³¹ To further study whether the change in the spin structure of La-doped Sr_2IrO_4 after electron doping leads to the sign reversal of PHE with temperature, we combined in-plane AMR measurements at 9 T. In Fig. 5, the AMR shows fourfold symmetry attributed to magnetocrystalline anisotropy, which has been illustrated in supplementary material S3.^{20,21} As the temperature rises from 20 to 70 K, the fourfold symmetry is weakened and ultimately transforms into twofold at around 90 K. The previous work²¹ has shown that this symmetry breaking of the La-doped Sr_2IrO_4 film is associated with changes in the spin structure. It is worth noting that the transition temperature of AMR is consistent with the temperature at which the PHE changes its sign. This implies that the

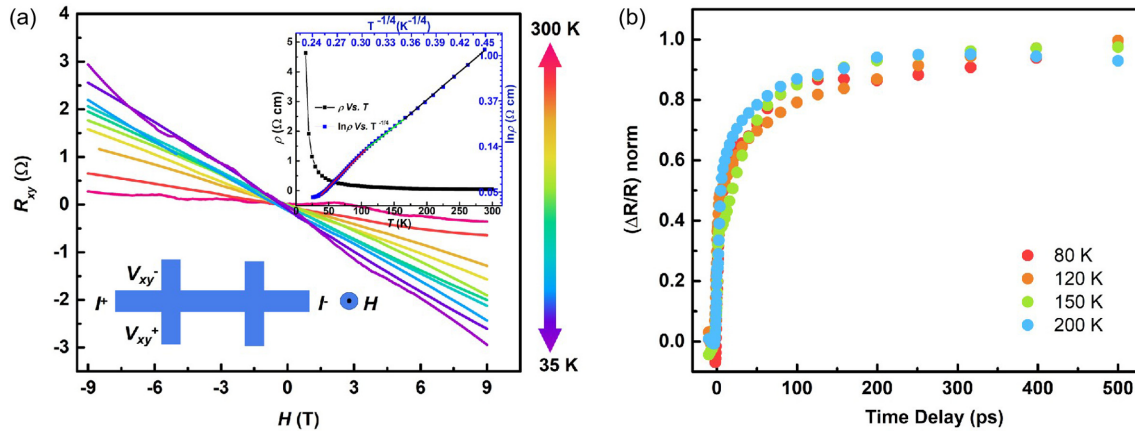


FIG. 4. (a) Traditional Hall measurements from 35 to 300 K and the schematic measurement setup. Upper right inset: the black data points denote the temperature dependence of resistivity, the blue data points denote $\ln \rho$ vs $T^{-1/4}$, and the solid lines are fitted by the 3D Mott-VRH thermal activation model. (b) Normalized time-resolved reflectivity traces ($\Delta R/R$) norm of the La-doped Sr_2IrO_4 film collected at 80, 120, 150, and 200 K.

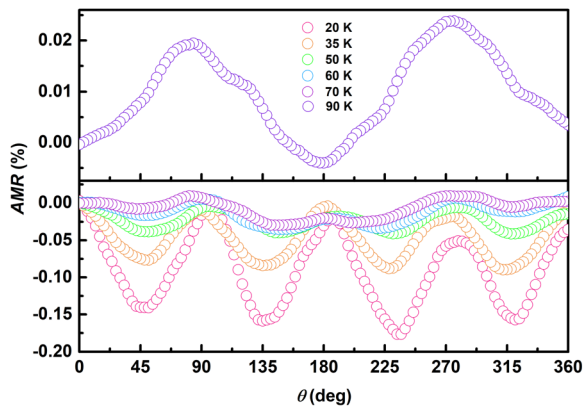


FIG. 5. In-plane AMR in a 9-T field at various temperatures.

sign reversal of PHE may be caused by the change in the spin structure. Doping of La reduces the rotation angle of the IrO_6 octahedra and affects the spin structure, which accounts for the reduction of in-plane ferromagnetism.⁸ As the temperature rises, such weak ferromagnetism in the La-doped Sr_2IrO_4 film is susceptible to thermal disturbances. When the temperature exceeds 80 K, the increasing thermal disorder obscures the long-range magnetic order, which leads to the sign reversal of PHE.

In order to have further insight into the physical reason behind the sign reversal temperature, we made in-plane AMR and PHE measurements for La-doped Sr_2IrO_4 films with 14 nm. Figure S6(a) in the supplementary material shows Laue oscillations around (0012) of 28-nm and 14-nm La-doped Sr_2IrO_4 films. As the film thickness decreases, the diffraction peak position of (0012) shifts to the right, indicating an enhancement of the in-plane tensile strain for the 14-nm La-doped Sr_2IrO_4 film. According to the previous report,⁴¹ tensile strain is expected to decrease the rotation angle of the IrO_6 octahedron and increase the Ir-O bond length and also plays a role in reducing the magnetism. As shown in Fig. S6(b), a sign reversal of R_{PHE} occurs but

approximately above 50 K. In the meantime, the AMR_{in} transforms from the fourfold symmetry into twofold [see the supplementary material [Fig. S6(c)]]. Compared with the results of the 28-nm La-doped Sr_2IrO_4 film, the reduction in the transition temperature is due to the reduction of ferromagnetic in samples with thinner thickness, which are more susceptible to thermal disturbances. Therefore, we suggested that the sign reversal of PHE occurs after La doping, even in films with different thicknesses, but the reversal temperature is related to the strength of ferromagnetism.

In addition, PHE is also related to the anisotropic s - d scattering, i.e., the conduction electrons are scattered into the localized d state by impurities.^{27,30,42} When the dominant s - d scattering process is $s\uparrow \rightarrow d\downarrow$ or $s\downarrow \rightarrow d\uparrow$, $R_{\parallel} > R_{\perp}$. In contrast, when the dominant s - d scattering process is $s\uparrow \rightarrow d\uparrow$ or $s\downarrow \rightarrow d\downarrow$, $R_{\parallel} < R_{\perp}$. Here, \uparrow and \downarrow denote spin up and spin down, respectively. The density of states of $d\uparrow$ and $s\uparrow$ at the Fermi energy level changes with increasing temperature, which enhances the scattering of $s\uparrow \rightarrow d\downarrow$ and $s\downarrow \rightarrow d\uparrow$ and leads to $R_{\parallel} > R_{\perp}$.³⁰ The specific change of s - d scattering for La-doped Sr_2IrO_4 films with temperature may also play an important role in the sign reversal of PHE. These results show that further experimental and theoretical study is required to provide deeper insight into the physical mechanism that governs this effect.

In summary, we have studied the temperature and magnetic field direction dependency of PHE in a La-doped Sr_2IrO_4 film. The amplitude of PHE increases approximately linearly with increasing H and is comparable with the giant PHE in ferromagnetic semiconductors. As the temperature increases, a sign reversal of angle-dependent PHE occurs at 90 K. Variable-temperature traditional Hall measurements and time-resolved optical studies indicate that the sign reversal is independent of the carrier type. The AMR measurements indicate that the sign reversal with temperature is probably due to changes in the spin structure. The reversal temperature is related to the strength of ferromagnetism. These unique properties compared to the PHE in undoped Sr_2IrO_4 films provide a platform for studying the magnetic properties of Sr_2IrO_4 films after electron doping and reveal an appealing possibility for the application of La-doped Sr_2IrO_4 films in spintronic and thermal switch magnetic sensor devices.

See the [supplementary material](#) for the magnetic properties of La-doped Sr₂IrO₄, the composition of the La-doped Sr₂IrO₄ film by SIMS measurements, the magnetic structure of La-doped Sr₂IrO₄ films, the relative magnitude of the PHE in the La-doped Sr₂IrO₄ film compared with other materials, the sheet carrier density n_s and carrier mobility μ for La-doped Sr₂IrO₄ films, and the influence of thickness on PHE for La-doped Sr₂IrO₄ films.

This work was supported by the National Key Research and Development Program of China (Grant No. 2021YAF0715600), the National Natural Science Foundation of China (Grant Nos. 62121005, 92065110, and 12204475), the Youth Growth Science and Technology Program of Jilin Province (Grant No. 20220508018RC), and the National Basic Research Program of China (Grant Nos. 2014CB920903 and 2013CB921701).

AUTHOR DECLARATIONS

Conflict of Interest

The authors have no conflicts to disclose.

Author Contributions

Mingrui Liu: Data curation (lead); Formal analysis (lead); Investigation (lead); Writing – original draft (lead); Writing – review and editing (lead). **Jianing Yue:** Time-resolved optical studies (lead). **Jianchao Meng:** Methodology (supporting). **Tingna Shao:** Films growth (supporting). **Chun-Li Yao:** Methodology (supporting). Funding acquisition (equal). **Xiaojuan Sun:** Writing – review and editing (supporting); Project administration (equal). **Jia-Cai Nie:** Writing – review and editing (supporting); Investigation (equal); Project administration (equal). **Dabing Li:** Project administration (lead).

DATA AVAILABILITY

The data that support the findings of this study are available within the article and its [supplementary material](#).

REFERENCES

- L. F. Mattheiss, *Phys. Rev. B* **13**, 2433 (1976).
- H. Zhang, C. Liu, X. Qi, X. Dai, Z. Fang, and S. Zhang, *Nat. Phys.* **5**, 438 (2009).
- X. Wan, A. M. Turner, A. Vishwanath, and S. Y. Savrasov, *Phys. Rev. B* **83**, 205101 (2011).
- R. Schaffer, E. K.-H. Lee, B. Yang, and Y. B. Kim, *Rep. Prog. Phys.* **79**, 094504 (2016).
- H. Watanabe, T. Shirakawa, and S. Yunoki, *Phys. Rev. Lett.* **110**, 027002 (2013).
- F. Wang and T. Senthil, *Phys. Rev. Lett.* **106**, 136402 (2011).
- M. Ge, T. F. Qi, O. B. Korneta, D. E. De Long, P. Schlottmann, W. P. Crummett, and G. Cao, *Phys. Rev. B* **84**, 100402(R) (2011).
- X. Chen, T. Hogan, D. Walkup, W. Zhou, M. Pokharel, M. Yao, W. Tian, T. Z. Ward, Y. Zhao, D. Parshall, C. Opeil, J. W. Lynn, V. Madhavan, and S. D. Wilson, *Phys. Rev. B* **92**, 075125 (2015).
- T. Han, D. Liang, Y. Wang, J. Yang, H. Han, J. Wang, J. Gong, L. Luo, W. K. Zhu, C. Zhang, Y. Zhang, and J. Supercond, *Nov. Magn.* **30**, 3493 (2017).
- H. Gretarsson, N. H. Sung, J. Porras, J. Bertinshaw, C. Dietl, J. A. N. Bruin, A. F. Bangura, Y. K. Kim, R. Dinnebier, J. Kim, A. Al-Zein, M. Moretti Sala, M. Krisch, M. Le Tacon, B. Keimer, and B. J. Kim, *Phys. Rev. Lett.* **117**, 107001 (2016).
- C. Cosío-Castaneda, G. Tavizon, A. Baeza, P. de la Mora, and R. Escudero, *J. Phys.:Condens. Matter* **19**, 446210 (2007).
- Y. Klein and I. Terasaki, *J. Phys.: Condens. Matter* **20**, 295201 (2008).
- O. B. Korneta, T. Qi, S. Chikara, S. Parkin, L. E. De Long, P. Schlottmann, and G. Cao, *Phys. Rev. B* **82**, 115117 (2010).
- Y. J. Yan, M. Q. Ren, H. C. Xu, B. P. Xie, R. Tao, H. Y. Choi, N. Lee, Y. J. Choi, T. Zhang, and D. L. Feng, “Electron-Doped Sr₂IrO₄: An Analogue of Hole-Doped Cuprate Superconductors Demonstrated by Scanning Tunneling Microscopy,” *Phys. Rev. X* **5**, 041018 (2015).
- D. Yao and T. Li, *J. Phys.:Condens. Matter* **30**, 495601 (2018).
- C. Dhital, T. Hogan, Z. Yamani, C. de la Cruz, X. Chen, S. Khadka, Z. Ren, and S. D. Wilson, *Phys. Rev. B* **87**, 144405 (2013).
- S. Boseggia, H. C. Walker, J. Vale, R. Springell, Z. Feng, R. S. Perry, M. M. Sala, H. M. Ronnow, S. P. Collins, and D. F. McMorrow, *J. Phys.:Condens. Matter* **25**, 422202 (2013).
- B. J. Kim, H. Jin, S. J. Moon, J. Y. Kim, B. G. Park, C. S. Leem, J. Yu, T. W. Noh, C. Kim, S. J. Oh, J. H. Park, V. Durairaj, G. Cao, and E. Rotenberg, *Phys. Rev. Lett.* **101**, 076402 (2008).
- C. Lu, S. Dong, A. Quindeau, D. Preziosi, N. Hu, and M. Alexe, *Phys. Rev. B* **91**, 104401 (2015).
- C. Lu, B. Gao, H. Wang, W. Wang, S. Yuan, S. Dong, and J. Liu, *Adv. Funct. Mater.* **28**, 1706589 (2018).
- M. R. Liu, H. X. Xue, J. C. Meng, R. P. Bai, W. M. Jiang, Z. Zhang, J. Z. Ling, L. He, C. M. Xiong, R. F. Dou, and J. C. Nie, *Phys. Rev. B* **100**, 075129 (2019).
- B. Ozer, H. Piskin, and N. Akdogan, *IEEE Sens. J.* **19**, 5493 (2019).
- T. Q. Hung, F. Terki, S. Kamara, K. Kim, S. Charar, and C. Kim, *J. Appl. Phys.* **117**, 154505 (2015).
- Y. Liu, J. Yang, W. Wang, H. Du, W. Ning, L. Ling, W. Tong, Z. Qu, G. Cao, Y. Zhang, and M. Tian, *Phys. Rev. B* **95**, 161103(R) (2017).
- A. V. Kudrin, O. V. Vikhrova, and Y. A. Danilov, *Tech. Phys. Lett.* **36**, 511 (2010).
- C. R. Akouala, R. Kumar, S. Punugupati, C. L. Reynolds, J. G. Reynolds, E. J. Mily, J. Maria, J. Narayan, and F. Hunte, *Appl. Phys. A* **125**, 293 (2019).
- T. R. Mcguire and R. I. Potter, *IEEE T. Magn.* **11**, 1018 (1975).
- M. Bowen, K. J. Friedland, J. Herfort, H. P. Schonherr, and K. H. Ploog, *Phys. Rev. B* **71**, 172401 (2005).
- T. Li, L. Zhang, and X. Hong, *J. Vac. Sci. Technol. A* **40**, 010807 (2022).
- S. Kokado, M. Tsunoda, K. Harigaya, and A. Sakuma, *J. Phys. Soc. Jpn.* **81**, 24705 (2012).
- M. Liu, H. Liu, T. Shao, W. Jiang, Z. Zhang, J. Ling, C. Yao, Y. Qiao, Q. Zhao, C. Xiong, R. Dou, and J. Nie, *Phys. Rev. B* **104**, 035301 (2021).
- X. Zhuo, J. W. Lai, P. Yu, Z. Yu, J. C. Ma, W. Lu, M. Liu, Z. Liu, and D. Sun, *Light: Sci. Appl.* **10**, 101 (2021).
- J. Ge, D. Ma, Y. Liu, H. Wang, Y. Li, J. Luo, T. Luo, Y. Xing, J. Yan, D. Mandrus, H. Liu, X. C. Xie, and J. Wang, *Nat. Sci. Rev.* **7**, 1879 (2020).
- A. Rajapitamahuni, L. Zhang, M. A. Koton, V. R. Singh, J. D. Burton, E. Y. Tsymbal, J. E. Shield, and X. Hong, *Phys. Rev. Lett.* **116**, 187201 (2016).
- H. X. Tang, R. K. Kawakami, D. D. Awschalom, and M. L. Roukes, *Phys. Rev. Lett.* **90**, 107201 (2003).
- Y. Bason, L. Klein, J. B. Yau, X. Hong, and C. H. Ahn, *Appl. Phys. Lett.* **84**, 2593 (2004).
- Y. Klein and I. Terasaki, *J. Electron. Mater.* **38**, 1331 (2009).
- N. Nagaosa, J. Sinova, S. Onoda, A. H. MacDonald, and N. P. Ong, *Rev. Mod. Phys.* **82**, 1539 (2010).
- C. Lu, A. Quindeau, H. Deniz, D. Preziosi, D. Hesse, and M. Alexe, *Appl. Phys. Lett.* **105**, 082407 (2014).
- H. Sharma, H. Bana, A. Tulapurkar, and C. V. Tomy, *Mater. Chem. Phys.* **180**, 5 (2016).
- S. Geprägs, B. E. Skovdal, M. Scheufele, M. Opel, D. Wermeille, P. Thompson, A. Bombardi, V. Simonet, S. Grenier, P. Lejay, G. A. Chahine, D. L. Quintero-Castro, R. Gross, and D. Mannix, *Phys. Rev. B* **102**, 214402 (2020).
- L. Zhou, B. C. Ye, H. B. Gan, J. Y. Tang, P. B. Chen, Z. Z. Du, Y. Tian, S. Z. Deng, G. P. Guo, H. Z. Lu, F. Liu, and H. T. He, *Phys. Rev. B* **99**, 155424 (2019).